XL CILAMCE
IBERO-LATIN AMERICAN CONGRESS ON COMPUTATIONAL METHODS IN ENGINEERING
NOVEMBER 11-14, 2019
Praiamar Natal Hotel & Convention
Natal, RN-BRAZIL

CONTINUOUS AND DISCONTINUOUS MODELING OF FAILURE FOR QUASI-BRITTLE MATERIALS

José Fabiano Araújo Moreira
Francisco Evangelista Junior
jf_moreira1991@hotmail.com
fejr.unb@gmail.com
Universidade de Brasília
Programa de Pós Graduação em Estruturas e Construção Civil, Prédio SG 12, primeiro andar Campus Darcy Ribeiro, Universidade de Brasília, 70910-900, Brasília, Distrito Federal, Brasil.
Abstract. This research aims to formulate and implement a continuous-discontinuous approach for failure of quasi-brittle materials. This approach is based on a damage evolution law using only physical parameters, which can be obtained through fracture and resistance tests without the need of further calibration. Comparison with experimental results were performed to assess the accuracy and efficiency. The tests simulated with the model were the three-point bending in a single edge notch beam. The results obtained herein confirmed the efficiency and accuracy of the model in predicting rupture behavior. Moreover, the model can provide results with equivalent accuracy to others in the literature using fewer elements in the mesh.

Keywords: Continuum Damage Mechanics, *Quasi*-brittle materials, Crack propagation, GFEM.

1 Introduction

In *quasi*-brittle fracture, the Fracture Process Zone (FPZ) ahead of the macrocrack is large when compared to the size of the crack and to the characteristic size of the structure [1, 2, 3, 4]. Most of this zone is characterized by a nonlinear behavior caused mainly by inelastic deformations and coalescence of microcracks, which is studied in the literature by Continuum Mechanics and Fracture Mechanics [5, 6, 7, 8, 9, 10]. Continuum Mechanics has been used to describe the dissipation behavior of materials induced by the initiation and development of microcracks around a macrocrack. One approach is the Continuum Damage Mechanics (CDM), which considers state variable to describe the irreversible processes, such as the state of damaging and softening [11, 12]. Fracture Mechanics deals with discontinuities caused by the formation and growth of a macrocrack. A very common idealization in Fracture Mechanics is the Cohesive Zone Models (CZM), initially introduced by Barenblatt [13, 14] and Dugdale [15], to overcome some limitations of the Linear Elastic Fracture Mechanism (LEFM) and to address the crack tip singularities.

Thus comes an idea of an integrated continuous/discontinuous failure description in which the degradation occurs initially in the FPZ described by a CDM and then the discontinuity growth described by Fracture Mechanics, when the damage reaches a limit value in order to demand the localization of a crack. Wells et al. [16]**,** Simone et al. [17], de Borst et al. [18]**,** Comi et al. [19], Cuvilliez et al. [20], Tejchman and Bobinski [21], Roth et al. [22] and Li and Chen [23] have successfully combined continuous-discontinuous approaches to model crack damage and propagation in two-dimensional domains. Some of these articles make use of the advantages of recently developed methods for crack propagation that use the Partition of Unit, such as the XFEM.

This article formulated and implemented a model that couples a continuous approach, through the damage mechanic and fracture laws, and a discontinuous approach, through the Generalized Finite Element Methods (GFEM), for the prediction of failures in *quasi*-brittle structures. Its main contribution is the development of a model able to simulate the resistance of structural members with mesh objectivity and crack propagations mesh independent. The novelty is a model based on a law of damage evolution with only physical parameters obtained in resistance and fracture tests without the need for additional calibration or curve fitting for the sample response curve, which allows the transition from the continuous to discontinuous with a compatible energy balance.

2 Damage model formulation

The proposed damage model is applied to the *quasi*-brittle materials under loading conditions that result in mode I or mixed (I+II) of crack propagation. The fundamental hypotheses which define the capacity and limitations of the model consider that: the material in process of damage evolution is considered an elastic medium and plastic and inelastic deformations are not considered; the damage is represented by a scalar variable $D (0 \leq D \leq 1)$, therefore, an isotropic damage condition is assumed for the material.

2.1 Control variable and activation criterion of damage

The damage is controlled by a state variable that is related to the strain tensor by an equivalent strain, ε_{eq}. For cases where there is a predominance of hydrostatic deformations and the local shear strain are negligible (mode I cracking), the equivalent strain presented by Mazars [24], here called ε_{eq}^{MA}, is suggested by literature as a simple and efficient measurement ([24, 25, 26, 17, 27, 4, 28]:

$$\varepsilon_{eq}^{MA} = \sqrt{\sum_{i=1}^{3} \left(\langle \varepsilon_i \rangle_+ \right)^2} \tag{1}$$

with $\langle \varepsilon_i \rangle_+ = (\varepsilon_i + |\varepsilon_i|)/2$ and ε_i the principal strain in the i direction.

In situations where shear stresses are not negligible in the definition of the strain state (mixed mode crack), the modified von Mises equivalent strain, ε_{eq}^{VM}, is a good alternative for the damage control variable [29, 25, 17, 30, 4, 28]:

$$\varepsilon_{eq}^{VM} = \frac{k-1}{2k(1-2\upsilon)} I_{\varepsilon 1} + \frac{1}{2k}\sqrt{\frac{(k-1)^2}{(1-2\upsilon)^2} I_{\varepsilon 1}^2 + \frac{6k}{(1+\upsilon)^2} J_{\varepsilon 2}} \tag{2}$$

where $I_{\varepsilon 1}$ is the fisrt invariant of the strain tensor, $J_{\varepsilon 2}$ is the second invariant of the deviatoric strain tensor, k is the ratio between compressive strength (f_c), and tensile strength (f_t) and υ is Poisson ratio.

2.2 Damage evolution law

The proposed model establishes that the specific energy (Φ_F) can be related to the fracture energy (G_F) by means of a characteristic length (l_c,) as initially proposed by Oliver [31]. Following this equivalence, the ratio σ-ε for the softening curve for the proposed continuum damage model is related to a finite-width region, i.e., l_c. Consequently, the scalar damage variable for the traction material is formulated based on a mode I cohesive fracture law, i.e., $D(\sigma\text{-}w) = D(\sigma\text{-}\varepsilon_{eq})$ with $w = \varepsilon_{eq} l_c$ and l_c being a characteristic length of element.

A softening law for the pure tension softening region can be described by a bilinear softening curve for conventional cementitious *quasi*-brittle materials (PCC), as suggested by Roesler et al. [32] and Evangelista Jr. et al. [33]. The fracture process zone can be described by a softening traction-displacement relation (σ-w) with its equivalence in σ-ε_{eq}. being shown in **Fig. 1**.

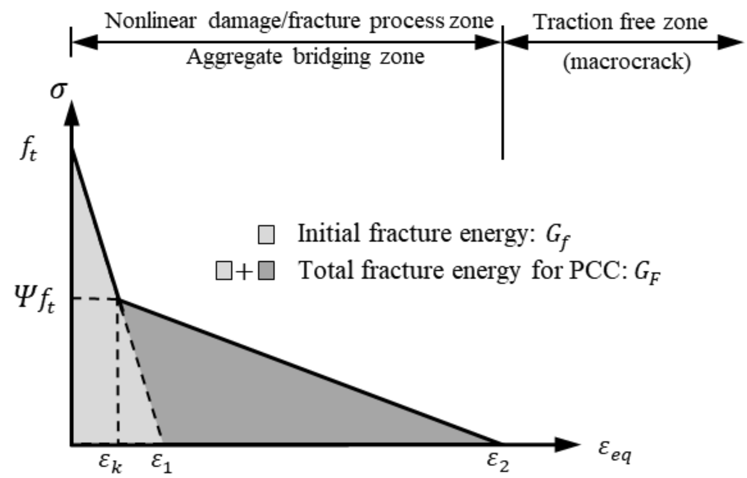

Fig. 1. Traction strain (σ-ε_{eq}) curve for damage evolution (adapted from Evangelista Jr. et al. [33]).

The parameters $\varepsilon_k, \varepsilon_1$, ε_2 and Ψ that define the damage law are solely based on material properties from fracture and resistance tests measured in laboratory, these parameters are G_f, G_F, $CTOD_c$ and f_t as defined in Wittman et al. [34], Bažant [35], Roesler et al. [32, 36], Park et al. [37] and Evangelista Jr. et al. [33].

3 Generalized Finite Element Method

The Generalized Finite Element Method (GFEM) was pioneered in the works of Babuška et al. [38], Duarte and Oden [39], Melenk and Babuška [40] and Oden et al. [41]. This method is based on the principle of Partition of Unity and consists in enhancing the traditional shape functions of finite elements with other so-called enrichment functions that better represent the local behavior of the solution. For the case of discontinuity, the enrichment function can be found from the kinematics of the displacement jump. The displacement field ($\boldsymbol{u}$) for an element can be interpolated by Eq. (3a), with $\boldsymbol{\mathcal{H}}_{\Gamma_d}$ being the Heaveside function centered at discontinuity Γ_d, and the displacement jump ($[\![\boldsymbol{u}]\!]$) in Γ_d given by Eq. (3b).

$$\begin{aligned} \boldsymbol{u} &= \boldsymbol{Na} + \boldsymbol{\mathcal{H}}_{\Gamma_d}\boldsymbol{Nb} \\ [\![\boldsymbol{u}]\!] &= \boldsymbol{Nb}|_{\Gamma_d} \end{aligned} \tag{3a,b}$$

where $\boldsymbol{a}$ and $\boldsymbol{b}$ are the regular and enhanced degrees of freedom, respectively.

For the constitutive relations, the tractions for the continuous domain are expressed in terms of the nodal displacements and the discontinuity stresses are expressed in terms of the additional nodal displacements, according to Eq. (4a-b), respectively:

$$\begin{aligned} \boldsymbol{\sigma} &= (1-\mathrm{D})\boldsymbol{D}_0\boldsymbol{\varepsilon} = (1-\mathrm{D})\boldsymbol{D}_0(\boldsymbol{Ba} + \boldsymbol{\mathcal{H}Bb}) \\ \boldsymbol{t} &= \boldsymbol{T}[\![\boldsymbol{u}]\!] = \boldsymbol{TNb} \end{aligned} \tag{4a,b}$$

where $\boldsymbol{B}$ is a matrix containing derivatives of shape functions, $\boldsymbol{\mathcal{H}}$ is the Heaviside function, $\boldsymbol{a}$ and $\boldsymbol{b}$ are, respectively, the standard and enriched degree of freedom vectors and $\boldsymbol{T}$ relates traction and displacements at the crack. In cohesive zone models, the relation $\boldsymbol{T}[\![\boldsymbol{u}]\!]$ is described by a constitutive model expressed in a traction versus crack opening curve that allows the simulation of the process zone by applying tractions to the opening plane depending on the crack opening value.

4 Numerical implementation

In the crack propagation process, when an element is cut by a crack, its nodes are than enriched. However, since there is a condition that the displacement jump at the crack tip must be zero, the nodes belonging to the element ahead of the crack tip are not enriched, even if their nodes belong to other elements that are crossed by the discontinuity. This strategy was successfully adopted in Wells and Sluys [42] and Simone [43]. In the discrete equation system of GFEM, the integration of some terms of stiffness matrix and force vector occurs only on a part of element domain. A special integration scheme is required to ensure that shape functions remain linearly independent. In the paper of Moës et al. [44]**,** Wells and Sluys [42] and Pereira et al. [45] it is proposed that the elements crossed by a discontinuity have their domains Ω^+ and Ω^- divided into subdomains. In each subdomain, the Gauss quadrature belonging to the adopted element is applied.

The propagation criterion is based on the value of the damage at the integration points of element ahead of the crack tip, so that at the end of a displacement increment, a discontinuity is inserted when the damage value at any integration point is close to one. Discontinuity is introduced as straight line within element.

For the propagation direction is used the direction of maximum accumulation of the non-local damage in a V-shaped window ahead of a discontinuity tip, similar to that proposed by Simone et al. [17].

A vector $\boldsymbol{r}_{\Gamma_d}$ in the direction of the crack propagation is calculated by:

$$\boldsymbol{r}_{\Gamma_d} = \sum_{i \in S} D_i w_i \frac{\boldsymbol{r_i}}{\|\boldsymbol{r_i}\|} \tag{5}$$

where S is the set of integration points i located within the region limited by the V-shaped, D_i is the value of damage at point i, $\boldsymbol{r_i}$ is the position vector in the direction of point i and w_i is a weight associated with the point i.

It is important to note the assumed equivalence for the dissipation of the fracture energy along l_c [31, 28]. However, in a context of finite element analysis, the mesh may have elements smaller or larger than the characteristic length. Therefore, a regularization procedure should be established in order to adapt the fracture energy of the characteristic length to the size of the mesh elements. This can be done by considering that l_c is equal to h_e of the finite element mesh, with its value given by L^e, $\sqrt[2]{A^e}$ or $\sqrt[3]{V^e}$, with L^e, A^e and V^e being respectively the length, area and volume of finite element.

5 Numerical simulations

Roesler et al. [32] performed three-point bending tests on small-scale concrete beams to determine fracture parameters and interpret the size effect on concrete. **Fig. 2** shows the geometry of the test with the geometric data of one of the beams tests $H = 150mm$, $S = 600mm$, $L = 700mm$ and $a_0 = 50mm$. The same fracture parameters adopted by Gaedicke and Roesler [46] and Roesler et al. [32] were used, their values were $G_F = 164.0\ N/m$, $G_f = 56.7\ N/m$ and $CTOD_C = 0.0186\ mm$. The material data were $E = 32\ GPa$, $\upsilon = 0.20$, $f_c = 58.3\ MPa$ and $f_t = 4.15\ MPa$. The simulation is done considering the plane stress state. The test control is performed by means of displacement increments at the point of force application (P), according to the experimental test. Simulations were performed with the continuous (*C*) and continuous-discontinuous (*C-D*) models with ε_{eq}^{MA} and ε_{eq}^{VM}. The finite element mesh used is shown in **Fig. 2**. The thickness was 80 mm and width of the notch adopted was two millimeters.

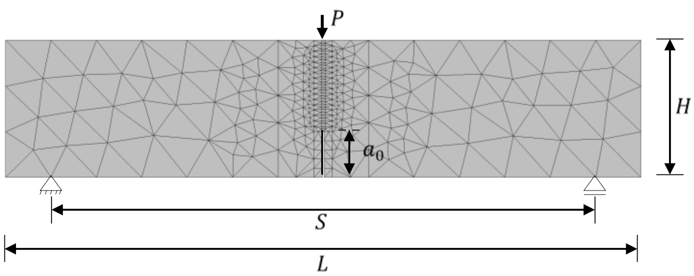

Fig. 2. Geometry and boundary conditions of TPB test. Finite element meshes with 581 elements.

Fig. 3 presents the experimental and numerical results and the respective comparisons of the curves relative to the applied force as a function of Crack Mouth Opening Displacement (CMOD). The results show that both proposed models were able to estimate with very good accuracy (maximum relative error of 5%), the maximum load (P_{max}) of the beam. It is important to note that the model achieved practically the same accuracy as the discontinuous model using a cohesive zone with interface elements of Gaedicke and Roesler [46], but with a very small number of elements (581 rather than 6285 used by Gaedicke and Roesler [46]). Comparing the curves obtained with ε_{eq}^{MA} and ε_{eq}^{VM} for the *C* case, it is seen that ε_{eq}^{MA} shows P_{max} slightly larger than ε_{eq}^{VM}. In the *C-D* case the propagation only occurs after P_{max}, so there is no difference for the estimates observed between the *C* and *C-D* models up to this point of the curve.

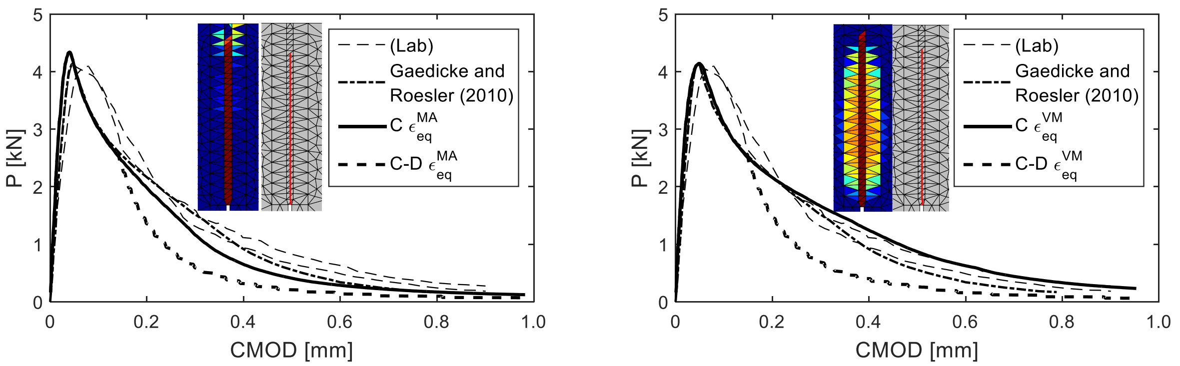

(a) (b)

Fig. 3. Comparison of experimental (Roesler et al. [32]) and numerical (Gaedicke and Roesler [46]) P-CMOD curves with results obtained for (a) ε_{eq}^{MA} and (b) ε_{eq}^{VM}.

It is observed that the bilinear law using ε_{eq}^{VM} presents slightly higher values for the post peak proposed model with softening curve in comparison to ε_{eq}^{MA}. It is important to note that although ε_{eq}^{VM} is defined for mixed-mode cases, it was also able to estimate the mode I cases. With respect to the *C-D* model, a decrease in the load capacity of the beam softening region is observed. This is because, in addition to the penalty of the mechanical properties of the material due to the damage model, the element has discontinuous displacements directly due to the presence of the crack by GFEM.

The damage distribution and crack propagation for the performed simulations are also shown in **Fig. 3**. As can be seen, the damaging zone using ε_{eq}^{VM} is slightly the one larger than ε_{eq}^{MA}. This is likely due to the calculation of ε_{eq}^{VM} is done using the strain tensor, and this takes into account the shear stress, the deformation criterion is reached in elements that would not be affected by the ε_{eq}^{MA}. It should be noted that although the distribution of damage is different, the overall response of structure is the same in mode I.

In order to show the mesh objective, it was performed simulations with three different mesh refinement. The simulations were carried out with the *C* model and ε_{eq}^{VM} equivalent strain. **Fig. 4** shows P-CMOD curves and damage distributions for these three meshes containing 269, 581 and 917 elements. As observed, the two most refined meshes present better results than the coarser mesh. This is due to better approximation of strain-stress field provided by the most refined mesh. However, the results show that the *C* model with regularization adopted which establishes the dissipation of fracture energy proportional to the characteristic length of the FE produces mesh objectivity, this is emphasized by the convergence of both P_{max} and softening curve between the meshes with 581 and 917 elements. With the proposed regularization for the *C* model, we noticed that even the results of very coarse meshes (269 elements) are fairly similar to the more accurate results provided by the refinement of the mesh for both P_{max} and softening curve.

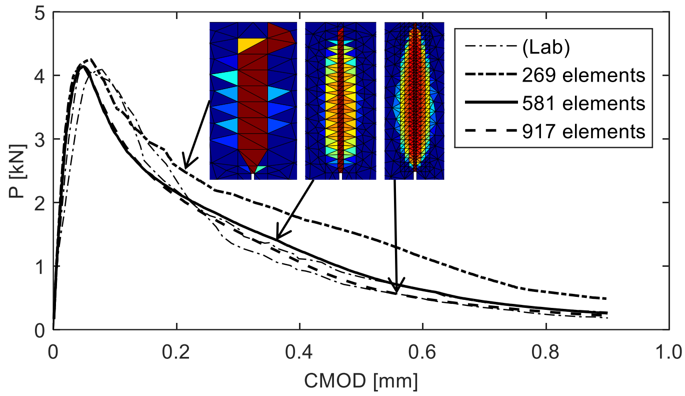

Fig. 4. Mesh objectivity: P-CMOD curve and damage distribution for different mesh refinement.

6 Conclusions

This work has formulated and implemented a continuous model, based on Damage Mechanics and fracture laws for damage evolution, and a continuous-discontinuous model (transition to fracture), which adds the XFEM/GFEM strategy to the previous model cited, for prediction of failures in structures of *quasi*-brittle materials. The models were validated by comparison with experimental results of the three-point bending in a single edge notch beam. The results obtained prove the efficiency and accuracy of the models in predicting with mesh objectivity the behavior of rupture of structure submitted to failure. The mode I predictions of P_{max} and the softening behavior using the ε_{eq}^{VM} are as good as the predictions with the ε_{eq}^{MA} that is idealized specifically for this failure mode.

The continuous model can achieve practically the same accuracy of results as other models found in the literature, even with a very small number of elements in the mesh. In addition, it uses only properties of small scale tests commonly performed in laboratory, without the need for any calibration of material properties and/or computational simulations. The continuous-discontinuous model and strategy with the use of GFEM confirmed the literature's observation that the prediction of the softening estimated by these models, although reasonably compared with the experiments, results in a decrease of load capacity in the softening region due to the presence of the finite element discontinuity.

Acknowledgements

To CNPq for the financial support.

References

[1] A. Hillerborg , M. Modeer and P. E. Peterson, "Analysis of crack formation and crack growth in concrete by means of fracture mechanics and finite elements," *Cement Concrete Research,* vol. 6, no. 6, pp. 773-782, 1976.

[2] Y. S. Jenq and S. P. Shah, "Nonlinear Fracture Parameters for Cement Based Concrete: Theory and Experiments," in *Application of Fracture Mechanics to Cementitiuos Composites*, S. P. Shah , Ed., 1985, p. 87–140.

[3] Z. P. Bažant and J. Planas, Fracture and Size Effect in Concrete and Other Quasibrittle Materials, London: CRC Press, 1998.

[4] M. Jirásek, "Damage and Smeared Crack Models," in *Numerical Modeling of Concrete Cracking*, G. Hofstetter and G. Meschke, Eds., Springer-Verlag Wien, 2011, pp. 1-49.

[5] C. Y. Hui, A. Jagota, S. J. Bennison and J. D. Londono, "Crack blunting and the strength of soft elastic solids," *Proceedings of the Royal Society A: Mathematical, Physical and Engineering Sciences,* vol. 459, no. 2034, pp. 1489-1516, 2003.

[6] A. Tarokh and A. Fakhimi, "Discrete element simulation of the effect of particle size on the size of fracture process zone in quasi-brittle materials," *Computers and Geotechnics,* vol. 62, pp. 51-60, 2014.

[7] D. Vavrik and I. Jandejsek, "Experimental evaluation of contour J integral and energy dissipated in the fracture process zone," *Engineering Fracture Mechanics,* vol. 129, pp. 14-25, 2014.

[8] K. Ha, H. Baek and K. Park, "Convergence of fracture process zone size in cohesive zone modeling," *Applied Mathematical Modelling,* vol. 39, no. 19, pp. 5828-5836, 2015.

[9] M. Fakoor and N. M. Khansari, "Mixed mode I/II fracture criterion for orthotropic materials based on damage zone properties," *Engineering Fracture Mechanics*, vol. 153, pp. 407-420, 2016.

[10] J. Xie, A. M. Waas and M. Rassaian, "Estimating the process zone length of fracture tests used in characterizing composites," *International Journal of Solids and Structures,* Vols. 100-101, pp. 111-126, 2016.

[11] L. Kachanov, Introduction to continuum damage mechanics, vol. 10, Dordrecht: Springer Netherlands, 1986, pp. X, 135.

[12] J. Lemaitre and J. L. Chaboche, Mechanics of Solid Materials, Cambridge University Press, 1994, p. 556.

[13] G. I. Barenblatt, "The formation of equilibrium cracks during brittle fracture. General ideas and hypotheses. Axially-symmetric cracks," *Journal of Applied Mathematics and Mechanics,* vol. 23, no. 3, pp. 622-636, 1959.

[14] G. I. Barenblatt, "The Mathematical Theory of Equilibrium Cracks in Brittle Fracture," *Advances in Applied Mechanics,* vol. 7, pp. 55-129, 1962.

[15] D. S. Dugdale, "Yielding of steel sheets containing slits," *Journal of the Mechanics and Physics of Solids,* vol. 8, no. 2, pp. 100-104, 1960.

[16] G. N. Wells, L. J. Sluys and R. de Borst, "Simulating the propagation of displacement discontinuities in a regularized strain-softening medium," *International Journal for Numerical Methods in Engineering,* vol. 53, no. 5, p. 1235–1256, 2002.

[17] A. Simone, G. N. Wells and L. J. Sluys, "From continuous to discontinuous failure in a gradient-enhanced continuum damage model," *Computer Methods in Applied Mechanics and Engineering,* vol. 192, no. 41-42, pp. 4581-4607, 2003.

[18] R. de Borst, J. J. C. Remmers, A. Needleman and M. A. Abellan, "Discretevs smeared crack models for concrete fracture: bridging the gap," *International Journal for Numerical and Analytical Methods in Geomechanics,* vol. 28, no. 7-8, pp. 583-607, 2004.

[19] C. Comi, S. Mariani and U. Perego, "An extended FE strategy for transition from continuum damage to mode I cohesive crack propagation," *International Journal for Numerical and Analytical Methods in Geomechanics,* vol. 31, no. 2, pp. 213-238, 2007.

[20] S. Cuvilliez, F. Feyel, E. Lorentz and S. Michel-Ponnelle, "A finite element approach coupling a continuous gradient damage model and a cohesive zone model within the framework of quasi-brittle failure," *Computer Methods in Applied Mechanics and Engineering,* Vols. 237-240, pp. 244-259, 2012.

[21] J. Tejchman and J. Bobiński , "Continuous and Discontinuous Modelling of Fracture in Plain Concrete under Monotonic Loading," in *Continuous and Discontinuous Modelling of Fracture in Concrete Using FEM,* Springer, Berlin, Heidelberg, 2013, pp. 109-162.

[22] S. N. Roth, P. Léger and A. Soulaïmani, "A combined XFEM–damage mechanics approach for concrete crack propagation," *A combined XFEM–damage mechanics approach for concrete crack propagation,* vol. 283, pp. 923-955, 2015.

[23] X. Li and J. Chen, "An extended cohesive damage model for simulating arbitrary damage propagation in engineering materials," *Computer Methods in Applied Mechanics and Engineering,* vol. 315, no. 1, pp. 744-759, 2017.

[24] J. Mazars, Application de la mécanique de l'éndommagement au comportementnon lineaire e à la rupture, Thèse de Doctorat d'État, Université de Paris VI, 1984.

[25] R. H. J. Peerlings, R. de Borst, W. A. M. Brekelmans and M. G. D. Geers, "Gradient-enhanced damage modelling of concrete fracture," *Mechanics of Cohesive-frictional Materials,* vol. 3, no. 4, pp. 323-342, 1998.

[26] E. Schlangen, Experimental and numerical analysis of fracture processes in concrete, Ph.D. Thesis, Delft University of Technology, 1993.

[27] S. P. B. Proenca and I. F. R. Torres, "Generalized finite element method for nonlinear three-dimensional analysis of solids," *International Journal of Computational Methods,* vol. 05, no. 01, pp. 37-62, 2008.

[28] M. Jirásek and M. Bauer, "Numerical aspects of the crack band approach," *Computers & Structures,* Vols. 110-111, pp. 60-78, 2012.

[29] J. H. P. de Vree, W. A. M. Brekelmans and M. A. J. van Gils, "Comparison of nonlocal approaches in continuum damage mechanics," *Computers & Structures,* vol. 55, no. 4, pp. 581-588, 1995.

[30] M. Jirásek and P. Grassl, "Evaluation of directional mesh bias in concrete fracture simulations using continuum damage models," *Engineering Fracture Mechanics,* vol. 75, no. 8, pp. 1921-1943, 2008.

[31] J. Oliver, "A consistent characteristic length for smeared cracking models," *International Journal for Numerical Methods in Engineering,* vol. 28, no. 2, pp. 461-474, 1989.

[32] J. R. Roesler, G. H. Paulino, K. Park and C. Gaedicke, "Concrete fracture prediction using bilinear softening," *Cement and Concrete Composites,* vol. 29, no. 4, pp. 300-312, 2007a.

[33] F. Evangelista Jr., J. R. Roesler and S. P. Proença, "Three-dimensional cohesive zone model for fracture of cementitious materials based on the thermodynamics of irreversible processes," *Engineering Fracture Mechanics,* vol. 97, pp. 261-280, 2013a.

[34] F. H. Wittmann, K. Rokugo, E. Brühwiler, H. Mihashi and P. Simonin, "Fracture energy and strain softening of concrete as determined by means of compact tension specimens," *Materials and Structures,* vol. 21, no. 1, pp. 21-32, 1988.

[35] Z. P. Bažant, "Concrete fracture models: testing and practice," *Engineering Fracture Mechanics,* vol. 69, no. 2, pp. 165-205, 2002.

[36] J. R. Roesler, G. H. Paulino, C. Gaedicke, A. Bordelon and K. Park, "Fracture Behavior of

Functionally Graded Concrete Materials for Rigid Pavements," *Transportation Research Record: Journal of the Transportation Research Board*, vol. 2037, pp. 40-49, 2007b.

[37] K. Park, G. H. Paulino and J. R. Roesler, "A unified potential-based cohesive model of mixed-mode fracture," *Journal of the Mechanics and Physics of Solids,* vol. 57, no. 6, pp. 891-908, 2009.

[38] I. Babuška, G. Caloz and J. E. Osborn, "Special Finite Element Methods for a Class of Second Order Elliptic Problems with Rough Coefficients," *SIAM Journal on Numerical Analysis,* vol. 31, no. 4, pp. 945-981, 1994.

[39] C. A. Duarte and J. T. Oden, Hp clouds – a meshless method to solve boundary value problem, Technical Report 9505, TICAM, University of Texas at Austin, 1995.

[40] J. M. Melenk and I. Babuška, "The partition of unity finite element method: Basic theory and applications," *Computer Methods in Applied Mechanics and Engineering,* vol. 139, no. 1-4, pp. 289-314, 1996.

[41] J. T. Oden, C. A. Duarte and O. C. Zienkiewicz, "A new cloud-based hp finite element method," *Computer Methods in Applied Mechanics and Engineering,* vol. 153, no. 1-2, pp. 117-126, 1998.

[42] G. N. Wells and L. J. Sluys, "A new method for modelling cohesive cracks using finite elements," *International Journal for Numerical Methods in Engineering,* vol. 50, no. 12, pp. 2667-2682, 2001.

[43] A. Simone, "Partition of unity-based discontinuous finite elements: GFEM, PUFEM, XFEM," *Revue européenne de génie civil,* vol. 11, no. 7-8, pp. 1045-1068, 2007.

[44] N. Moës, J. Dolbow and T. Belytschko, "A finite element method for crack growth without remeshing," *International Journal for Numerical Methods in Engineering,* vol. 46, no. 1, pp. 131-150, 1999.

[45] J. P. Pereira, C. A. Duarte, D. Guoy and X. Jiao, "hp-Generalized FEM and crack surface representation for non-planar 3-D cracks," *International Journal for Numerical Methods in Engineering*, vol. 77, no. 5, pp. 601-633, 2009.

[46] C. Gaedicke and J. R. Roesler, "Fracture-Based Method to Determine Flexural Capacity of Concrete Beams on Soil," *Road Materials and Pavement Design,* vol. 11, no. 2, pp. 361-385, 2010.